Bull. Chem. Soc. Ethiop. **2024**, 38(5), 1413-1427.
DOI: https://dx.doi.org/10.4314/bcse.v38i5.17

ISSN 1011-3924
Printed in Ethiopia
Online ISSN 1726-801X

DUAL FLUORESCENCE EMISSION OF *p*-N,N-(DIALKYLAMINO) BENZYL-IDENEMALONONITRILE AND RELATED SYSTEMS: EVIDENCE FOR DIRECT EXCITATION OF GROUND STATE TWISTED INTRAMOLECULAR CHARGE TRANSFER (TICT) CONFORMER

Desta G. Woldegiorgis[1], Ephriem T. Mengesha[1*], Neelaiah Babu G.[1], Maria Susai Boobalan[1], Taye B. Demissie[2] and Endale Teju[1]

[1]Department of Chemistry, CNCS, Haramaya University, Haramaya, P.O. Box 138, Dire Dawa, Ethiopia
[2]Department of Chemistry, University of Botswana, Notwane Rd, P/bag UB 00704 Gaborone, Botswana

(Received July 17, 2023; Revised May 12, 2024; Accepted May 15, 2024)

ABSTRACT. The mechanism of dual fluorescence emission of a fluorophore is controversial ever since its first observation in *p*-N,N-dimethylaminobenzonitrile (DMABN). Excited state twisted intramolecular charge transfer (TICT) and planarized intramolecular charge transfer (PICT) models have been the two prominent theories used to explain the dual fluorescence mechanism in several systems. These mechanisms are based on excited state adiabatic structural changes of the fluorophore. Nevertheless, pieces of evidences based on excitation spectral measurements at different emission windows suggest the possibility of additional and/or alternative mechanisms based on ground state structural changes of the fluorophore. In this paper, we have presented a systematic steady-state absorption and fluorescence spectroscopy of a donor-πacceptor system, *p*-N,N-(dialkylamino)benzylidenemalononitrile, and related compounds in solvents of different polarities. The excitation spectrum of *p*-N,N-(dialkylamino) benzylidenemalononitrile is found to be dependent on the emission window. Furthermore, the emission spectra of the molecule are dependent on the excitation wavelength which suggest that the molecule consists of two stable ground state conformational isomers. The spectroscopic pieces of evidence together with results from DFT calculations are in favor of the solvent-induced ground state structural change of the fluorophore. Hence, two ground state conformers of *p*-N,N-(dialkylamino)benzylidenemalononitrile are attributed to the dual emission of the molecule.

KEY WORDS: Dual fluorescence, Charge transfer, TICT, PICT, Excitation, Benzylidenemalononitriles

INTRODUCTION

Intramolecular charge transfer (ICT) is a process of significant charge delocalization in molecules containing electron donating group (D) and electron-accepting group(A) connected by π-linkers (D-π-Acceptor). This process is highly modulated by the strength of the donor, the acceptor and solvent environment. ICT is a common phenomenon in nature and is a crucial step in many biological processes [1].

The observation of intramolecular charge transfer in 4-(dimethylamino) benzonitrile (DMABN) by Lippertand co-workers in polar aprotic solvents has initiated immense interest among the scientific community because of the potential application taking advantage of the process. On one hand, understanding and modulation of the ICT process is crucial in the rational design and development of materials for technological applications such as optoelectronic materials, non-linear optics, viscosity sensors and pH and polarity sensors [2-6]. On the other hand, the observation of dual fluorescence in DMABN in polar aprotic solvents [7] and the mechanism by which it occurs remained an interesting topic of debate among different scientific groups as it presents an obvious exception from the Kasha's rule [8].

*Corresponding authors. E-mail: eph121983@gmail.com

Dual fluorescence is a phenomenon where a single molecule gives rise to a single emission from a locally excited state (LE emission) in non-polar solvents, while two fluorescent emissions (one from the locally excited state and the other anomalous band from the charge transfer state (CT emission)) in polar aprotic solvents [9-11]. Over the years, several donor-pi-acceptor systems including DMABN have been investigated in order to elucidate the mechanism for the anomalous emission. The explanations ranged from the formations of excited state complexes (exciplexes) [12-14] to adiabatic structural changes in the excited state [15-18] were forwarded as possible source of the anomalous CT emission. In the latter category, the twisted intramolecular charge transfer (TICT) model and planar intramolecular charge transfer (PICT) models stood out. In the TICT model proposed by Grabowski and co-workers [15-18], a 90° twisting motion of the dimethyl amino group along the C-N bond accompanied by complete charge transfer is put as requirement for the formation of the charge transfer state. In this respect, Dobkowski and co-workers [18] showed that dual fluorescence of 2-(N-methyl-N-isopropylamino)-5-cyanopyridine in methanol is accompanied by syn-anti isomerization around the C-N bond, supporting the TICT hypothesis.

On the other hand, Zachariasse and co-workers proposed the PICT model [19-21], which states that a small energy gap between the locally excited state and the charge transfer states, allowing solvent induced pseudo-Jahn-Teller coupling between the states is the requirement. This coupling is affected by the out-of-plane inversion mode of the amino nitrogen [22, 23]. This argument is supported by the absence of dual fluorescence in rigid planar aminobenzonitriles1-methyl-5-cyanoindoline(NMCI) and l-methyl-6-cyano-l,2,3,4-tetraquinoline (NMCQ), in which the 5-membered or6-membered ring connecting the amino nitrogen with the phenyl group hinders the nitrogen inversion; while NMCB with a 7-membered ring, ICT and dual fluorescence again starts to appear [21]. More evidence against the TICT model is provided by Yoshihara and co-workers [24] from the observation of dual fluorescence in fluorazene (FPP), a molecule incapable of twisting motion. Even though this observation is presented against the TICT model, it can also be used as evidence against the PICT model as FPP is a rigid planar aminobenzo-nitriles which is not supposed to show dual emission because of hindered nitrogen inversion according to the PICT model. Another important observation from their result [24] is that, unlike DMABN with both dialkylamino donor moiety and strong cyano acceptor moiety, FPP lacks the acceptor moiety and yet still capable of showing dual emission in polar aprotic solvents. The implication of such observation is either, the acceptor moiety is not a necessary condition or the benzene ring is acting as an acceptor.

The common feature of the TICT and PICT models discussed above is attribution of the source of dual emission entirely to the excited state conformational changes with little or no consideration of the possibility of conformational dynamics in the ground state. In the last decade, an alternative explanation for the anomalous emission of DMABN and related compounds is reported in the literature [25-28] from the perspective of ground state structural changes. Based on excitation spectra measurements of the compounds at different emission windows, along with excitation wavelength dependence of the relative intensities of the LE and CT emissions, two ground state conformers of the same compound were suggested. In this respect, strong independent experimental evidence for two ground state conformers of DMABN was suggested by Yasiri and co-workers [29] based on single-molecule electrical conductance measurement where no photoexcitation is involved. They showed two conductance values attributed to the planar and polar solvent stabilized twisted conformers of DMABN. In light of the above observations, the main objective of the present work is systematic investigation of fluorescent properties of p-N,N-(dialkylamino)benzylidenemalononitrile and related benzylidenemalononitrile derivatives (molecular structures presented in Figure1) in solvents of different polarities by considering both ground state and excited state conformational dynamics. Hence this study attempts to provide additional and/or alternative mechanisms of dual fluorescence based on ground-state conformational changes of the fluorophore. These classes of compounds have been studied as

"molecular rotors" in order to probe solvent friction [30] and polarity [31], as fluorescent probes of microviscosity of lipid bilayers and polymer environments [32] and as nonlinear optical devices owing to their large hyperpolarizability [4] to mention a few.

All three systems considered possess a strong dicyanovinyl acceptor moiety with different strengths of the donor moiety. As explained in the coming sections, these systems help to test several aspects of the hypothesis of two ground state conformers being responsible for the dual emission. Structure II for example is similar to DMABN except that, instead of the cyanoacceptor group, the compound contains stronger dicyanovinyl acceptor moiety which enhances structural changes involving charge transfer both in the ground S_0, and excited S_1 states.

The implication is unlike DMABN which shows single absorption (and later revealed as a combination of two distinct but very similar excitation spectra) band near 300 nm [25], two distinct absorption bands that independently could be excited to fluorescent states are expected for this system. Hence this study helps to clarify the hypothesis of existence of two stable equilibrium ground state structures Prof. proposed by prof. M. Redi-Abshiro's group [25-28].

EXPERIMENTAL

Experimental details

The synthetic procedure of benzylidenemalononitriles (compounds **I-III**) is reported elsewhere [33]. Briefly, to an equimolar mixture of malononitrile and arylaldehyde, water was added (20 v/w) and stirred for 15 min. The solid produced was isolated by simple filtration and dried. The solid product was recrystallized by hot ethanol. The products were characterized by NMR (^{1}H and ^{13}C) and the melting points were compared with the reported literature.

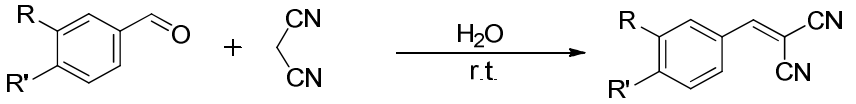

Compounds (I -III)

	R	R'
Structure I	H	H
Structure II	H	$N(CH_3)_2$
Structure III	OCH_3	OH

2-Benzylidenemalononitrile (Compound **I**) [33]: 93% Yield; m.p.: 83 ^{0}C; ^{1}H NMR (400 MHz, $CDCl_3$): δ 7.89 (d, J = 7.8 Hz, 1H), 7.77 (s, 1H), 7.61 (m, 1H), 7.53 (m, 1H); ^{13}C NMR (100 MHz, $CDCl_3$): δ 159.9, 134.6, 130.9, 130.7, 129.6, 113.7, 112.5, and 82.9.

2-(4-(Dimethylamino)benzylidene)malononitrile (Compound **II**) [34]: 90% Yield; m.p.: 180 ^{0}C; ^{1}H NMR (400 MHz, $CDCl_3$): δ 7.79 (d, J = 9.0 Hz, 2H), 7.44 (s, 1H), 6.67 (d, J = 9.1 Hz, 2H), 3.13 (s, 6H); ^{13}C NMR (100 MHz, $CDCl_3$): δ 158.1, 154.2, 133.7, 119.3, 115.9, 114.8, 111.6, and 40.0.

2-(4-Hydroxy-3-methoxybenzylidene)malononitrile (Compound **III**) [35]: 95% Yield; m.p.: 148 ^{0}C; ^{1}H NMR (400 MHz, $CDCl_3$): δ 7.92 (s, 1H), 6.98-7.32 (m, 3H), 6.02 (s, 1H), 3.86 (s, 3H). ^{13}C NMR (100 MHz, $CDCl_3$): δ 161.8, 152.2, 148.4, 128.4, 128.2, 116.8, 113.5, 110.4, 81.8, and 55.3.

Absorption and fluorescence spectra of the test molecules were measured in spectroscopic grade solvents of various polarities (n-hexane, cyclohexane, 1,4-dioxane, dichloromethane, and acetonitrile) at room temperature ca. 25 ^{0}C using SPECTRONIC GENESYS 2PC UV-Vis

spectrophotometer and Shimadzu RF 5301PC spectrofluorimeter, respectively, with a resolution of 1 nm. In all cases, 1 cm quartz cuvettes were utilized. In order to decrease the effect of aggregation and inner filter effects, the optical density values for absorption and fluorescence measurements were kept in the vicinity of 1 and 0.1, respectively. For fluorescence excitation and emission spectral measurements, the first order and second order Rayleigh scattering signals were removed to accentuate the fluorescence signals.

Computational details

Quantum chemical calculations were carried out to support the experimental results. Computation of the molecules were carried out using Gaussian09W quantum chemistry program package [36] using Density functional theory (DFT), B3LYP functional together with the 6-31G(d,p) basis set [36-38]. Global minimum geometries were confirmed by frequency calculations, where calculated frequencies for all systems were positive. The vertical excitation of the molecular systems has been computed using time-dependent density functional theory (TD-DFT) [39] using B3LYP functional and 6-31G(d,p) basis set. The role of solvent effects was carefully investigated using the polarizable continuum model (PCM) under its integral equation formalism (IEF-PCM). The solvent effect has been carefully examined on both excited and ground state geometries using different solvents: Cyclohexane (CH_X), acetonitrile (ACN), and dichloromethane (DCM).

RESULTS AND DISCUSSION

Absorption spectra

Experimental absorption spectra of structures **I** (black), **II** (red) and **III** (blue) in n-hexane solutions are presented in Figure 1. While both structures, **I** and **II**, show similar features in the vicinity of 320 nm, structure **II** showed an additional largely red-shifted absorption near 420 nm. Considering the structural similarity between **I** and **II**, the second absorption band in **II** could be assigned as a structural isomer as a result of donor *p*-N,N-dimethylamino substitution. Such substitution potentially brings two possible structural isomers relative to the neutral planar form: Zwitterionic structure and conformational isomer due to twisting motion of the dimethylamino moiety relative to the benzene ring. It is important to note that even though there is potentially additional conformation via rotation of the dicyanovinyl acceptor moiety, this possibility is excluded as we did not observe any conformational isomer in structure **I**.

In order to further understand the source of the second band, the absorption spectrum of another structurally related compound (**III**) was measured in the same solvent (Figure 1 blue curve). The molecule shows one broad absorption spectrum centered near 350 nm with some vibronic structures which is expected in non-polar solvents. Unlike structure **II**, the donor group in structure **III** has restricted conformation because of the hydrogen bonding with the neighboring methoxy group. The presence of this H-bond is evidenced from smaller calculated (B3LYP/6-31G (d,p)) O-H stretching frequency (3753 cm^{-1}) relative to phenol system, 3822 cm^{-1}. Therefore, it is possible to suggest that the source of the second red-shifted absorption band in structure **II** is due to conformation of the *p*-dimethylamino moiety. Hence, there are two possible conformational isomers of structure **II** in the ground state.

Solvent effects on the absorption spectra of structures **I** (Figure 2a) and **II** (Figure 2b) have also been investigated in solvents of various polarities and the results are presented in Figures 2a and 2b, respectively.

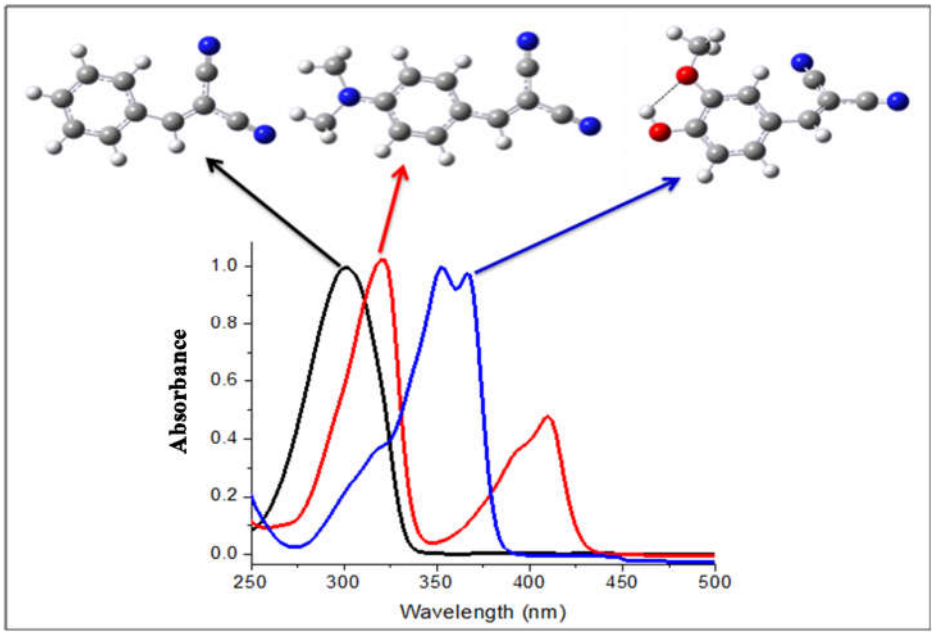

Figure 1. The experimental absorption spectrum of structure (**I**) (black), structure **II** (red) and structure **III** (blue) in n-hexane solution. For easier comparison, the spectra are normalized with respect to their absorption maxima.

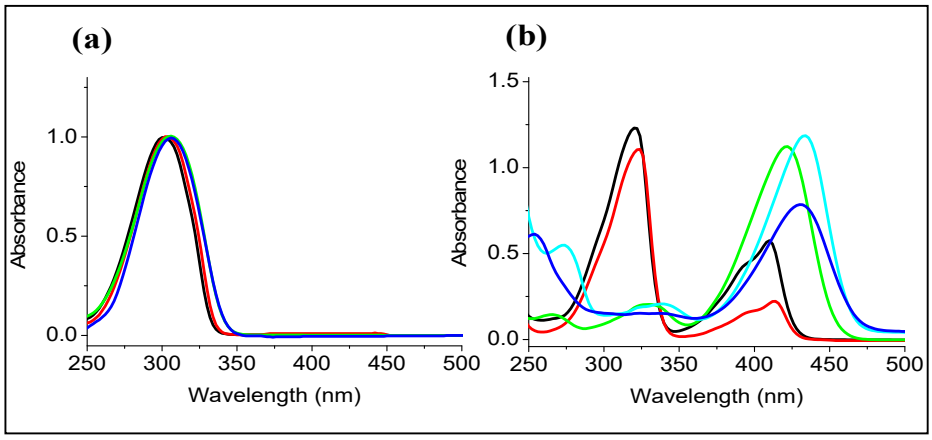

Figure 2. The experimental absorption spectrum of structure **I** (a) and structure **II** (b) in solvents of various polarities. n-Hexane (black), cyclohexane (red), dichloromethane (cyan) and acetonitrile (blue).

The absorption maximum of structures **I** is changed from 300 nm in n-hexane to 308 nm in acetonitrile ($\Delta\lambda$ = 8 nm) showing small bathochromic shift. Similarly, the absorption maxima of

structure **II** changed from 320 nm and 410 nm in n-hexane to 335nm and 430 nm in acetonitrile, corresponding to Δλ values of 15 nm and 20 nm for the first and second absorption bands, respectively. The spectra in both structures generally show bathochromic shifts suggesting increase of the excited state dipole moments of the two molecules. The shift is, however, larger in structure **II** because of the presence of the dimethyl amino donor moiety. Structure **II** also shows an interesting solvation effect. In non-polar solvents, two distinct absorptions near 320 and 420 nm are observed with larger relative intensity for the first absorption band. The situation changes, however, with increasing the polarity of the solvent. In polar solvents (for instance acetonitrile), the first absorption band almost disappears while the red-shifted absorption becomes the dominant absorption. The results suggest preferential stabilization of the red absorbing conformer in more polar solvents. Values of the absorption, excitation and emission maxima of structures **I** and **II** in solvents of different polarities are presented in Tables 1 and 2, respectively.

Table 1. Experimental values of the absorption, excitation and emission maxima of structures **I** and **II** in solvents of different polarities.

Structure **I**	Solvent	Δ*f**	Abs (nm)	Em_1	
	n-Hexane	-0.0014	300	322	
	Cyclohexane	-0.0018	302	335	
	1,4-Dioxane	0.0205	306	**342**	
	Dichloromethane	0.2127	310	335	
	Acetonitrile	0.3060	308	341	

Structure **II**	Solvent	Δ*f**	Abs 1	Abs 2	Em_1	Em_2
	n-Hexane	-0.0014	320	410		
	Cyclohexane	-0.0018	324	413	346	446
	1,4-Dioxane	0.0205	330	422	358	460
	Dichloromethane	0.2127	338	434	384	474
	Acetonitrile	0.3060	335	430	383	532

$$*\Delta f = \left(\frac{\varepsilon-1}{2\varepsilon+1} - \left(\frac{n^2-1}{2n^2+1}\right)\right)$$

Note that emission is measured via excitation near the absorption maxima. Δf, ε and n, refers to the solvent polarity function, dielectric constant and refractive index of the solvent.

Emission spectra

In the previous section, analyses of solvent dependent absorption spectral results suggested that structure **II** exists in two conformational isomers. In this section the fluorescence properties of this molecule from selective excitation of each absorption bands will be investigated. The emission spectra of structure **I** and **II** in solvents of different polarities are presented in Figures 3a and 3b, respectively.

In line with the Kasha rule, structure I shows a single emission band centered at 330 nm in all solvents with a small bathochromic shift, $\Delta\lambda\sim$ 19 nm (see Table 2) evidencing a smaller change in dipole moment upon excitation. This is typical of LE emission from a Franck-Condon state. On the other hand, two emission bands centered at 370 nm and 470 nm are observed via excitation in the vicinity of the first absorption band of structure **II**. The first emission band of structure **II** has similar features with the emission of structure **I** (although with larger bathochromic shift of 37 nm in **II** in n-hexane) and could be generally assigned as LE emission. However, the second emission band of structure II shows a large bathochromic shift (Δλ = 86 nm) where the emission maximum shifts from 446 nm in cyclohexane to 532 nm in acetonitrile. The large bathochromic shift suggests high charge transfer character of the second emitting state. Hence, the second red

shifted emission could be assigned as an emission from a TICT state. This conclusion is made considering the absence of the second emission band in the structurally related 9-(dicyanovinyl)-julolidine (DCVJ) with a donor group which is not capable of twisting motion [31].

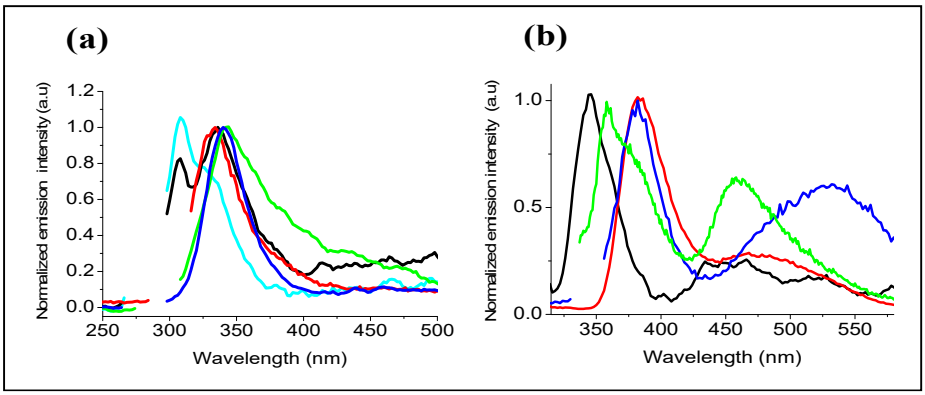

Figure 3. Peak normalized emission spectra of (a) structure **I** and (b) structure **II** in solvents of different polarities (n-hexane, cyan; cyclohexane, black; 1,4-dioxane, green; dichloromethane, red; and acetonitrile, blue.). For both structures, the excitation wavelength is in the vicinity of 300 nm. Note that for structure **II** the excitation wavelength corresponds to the first absorption band. Resonance Rayleigh scattering signal is removed from the spectra

Despite the fact that structure **II** gives a well-separated absorption signal for each conformer, selective excitation of the first band still gives two emissions. Two possible reasons for the red shifted TICT emission could be proposed: either (**I**) the emitting TICT state is populated from the LE state via excited state conformational dynamics within the fluorescence lifetime of the LE state or (ii) the S_0-S_n ($n \geq 2$) transition of the TICT conformer overlaps with the S_0-S_1 transition of the non-twisted (planar) conformer and hence co-excitation of the two forms. Excitation wavelength dependence of the emission spectrum of structure **II** was further tested in dichloromethane solution and the results are presented in Figure 4(a).

The emission spectrum of structure **II** shows significant dependence on the excitation wavelength. Excitation at 300 nm shows dual emission, while red-edge excitation (excitation at 400 nm) shows a single emission confirming selective excitation of the twisted ground state conformer. It is also worth noting that direct access of the excited state twisted conformer is also possible from the excitation of the ground state TICT conformer.

Further evidence about the source of the two emitting states of structure **II** comes from the measurement of excitation spectra at different observation windows. In this respect, we have presented in Figure 4(b) the excitation spectra of structure **II** at observation windows corresponding to the LE (black curve) and CT emissions (red curve). The result shows two different excitation spectra are observed for different observation windows confirming the presence of two structures in the ground state. The results also show that the absorption spectrum contains contributions from both excitation spectra. This argument is in line with the results from the absorption spectral measurements, the existence of two stable ground state conformers.

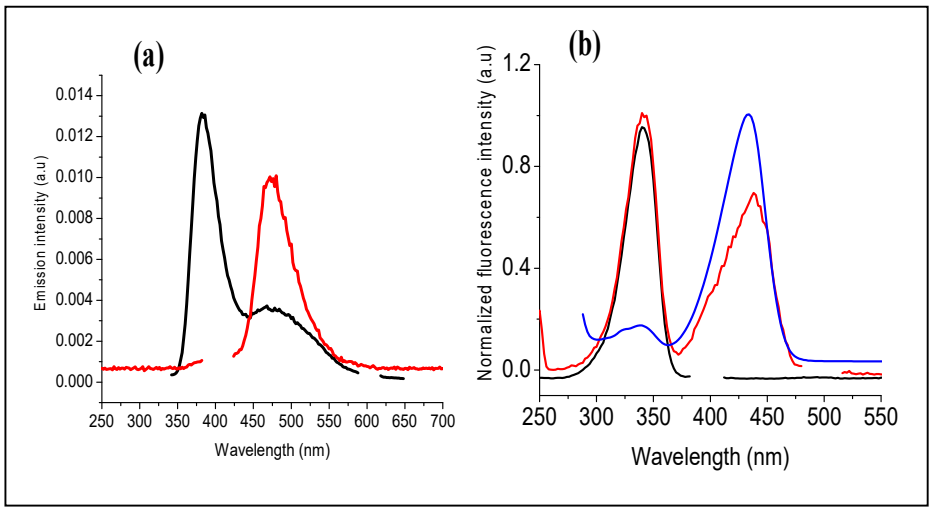

Figure 4. (a) Emission spectrum of structure **II** at excitation wavelength 300 nm (black, left) and 400 nm (red, right) in dichloromethane solution. Note that first order and second order Rayleigh scattering signals are removed from the spectra. (b) Peak normalized excitation spectra of structure **II** in dichloromethane monitored at emission wavelength windows of 400 nm (black) and 500 nm (red). Absorption spectrum of the compound in dichloromethane solution is also presented (blue) for comparison. Scattering signals are removed from the spectra.

Solvatochromism and Stocke's shift analyses

Solvatochromism [40, 41] has been established as a readily applicable and powerful tool to investigate the local polarity in macrosystems or even the conformation and binding of proteins [42, 43]. In this section, Lippert–Mataga equations (Eq. 1-3) were applied for quantitative analyses of the solvatochromic effects and associated Stocke's shifts observed in structure **II** [43-46]. Although there are several models developed for solvatochromic and associated dipole moment analyses, the Lippert-Mataga equation was selected as it provides better dipole moment value in solvent systems whose quality is comparable to results from more accurate Stark-effect measurements at least for the push-pull system, para-aminobenzoicacid (PABA) [47]. The results are presented in Figure 5(a-d).

$$\tilde{\nu}_A = \tilde{\nu}_A^0 - \frac{2\mu_g(\mu_e-\mu_g)}{4\pi\varepsilon_0 hca^3}\left[\frac{\varepsilon_r-1}{2\varepsilon_r+1} - \left(\frac{n^2-1}{2n^2+1}\right)\right] \quad (1)$$

$$\tilde{\nu}_F = \tilde{\nu}_F^0 - \frac{2\mu_e(\mu_e-\mu_g)}{4\pi\varepsilon_0 hca^3}\left[\frac{\varepsilon_r-1}{2\varepsilon_r+1} - \left(\frac{n^2-1}{2n^2+1}\right)\right] \quad (2)$$

$$\tilde{\upsilon}_A - \tilde{\upsilon}_F = \frac{2}{4\pi\varepsilon_0 hc}\left(\frac{\varepsilon-1}{2\varepsilon+1} - \frac{n^2-1}{2n^2+1}\right)\frac{(\mu_e-\mu_g)^2}{a^3} + K \quad (3)$$

where $\Delta f = \left(\frac{\varepsilon-1}{2\varepsilon+1} - \frac{n^2-1}{2n^2+1}\right)$ represents the measure of the solvent polarity function, $\widetilde{\upsilon_A}$ and $\widetilde{\upsilon_F}$ are the energy of the absorbance and emission maximum in wave-numbers, $\tilde{\nu}_A^0$ and $\tilde{\nu}_F^0$ are absorption

and emission wavenumbers in a vacuum, respectively; μ_g and μ_e is the dipole moment in the ground and excited singlet state, respectively, ε is the solvent dielectric constant,n is the solvent refractive index, ε_o is the permittivity of vacuum is the solvent refractive index, h being Planck's constant and c, the velocity of light in vacuum; a is the radius of the molecule which is estimated to be 6.0 Angstroms.

From the first absorption and first emission bands, the slope analyses give a ground state (μ_{g1}) and excited state (μ_{e1}) dipole moments of 9.3 and 20.4 D, respectively. Hence the change in dipole moment upon excitation of the first conformer becomes 11.1 D. Similarly, the values of the ground (μ_{g2}) and excited state (μ_{e2}) dipole moments are found to be 7.1 and 19.5 D, respectively, for the second conformer which gives a change of 12.4 D upon excitation. The results show that both conformers are polar with large charge transfer characteristics upon excitation.

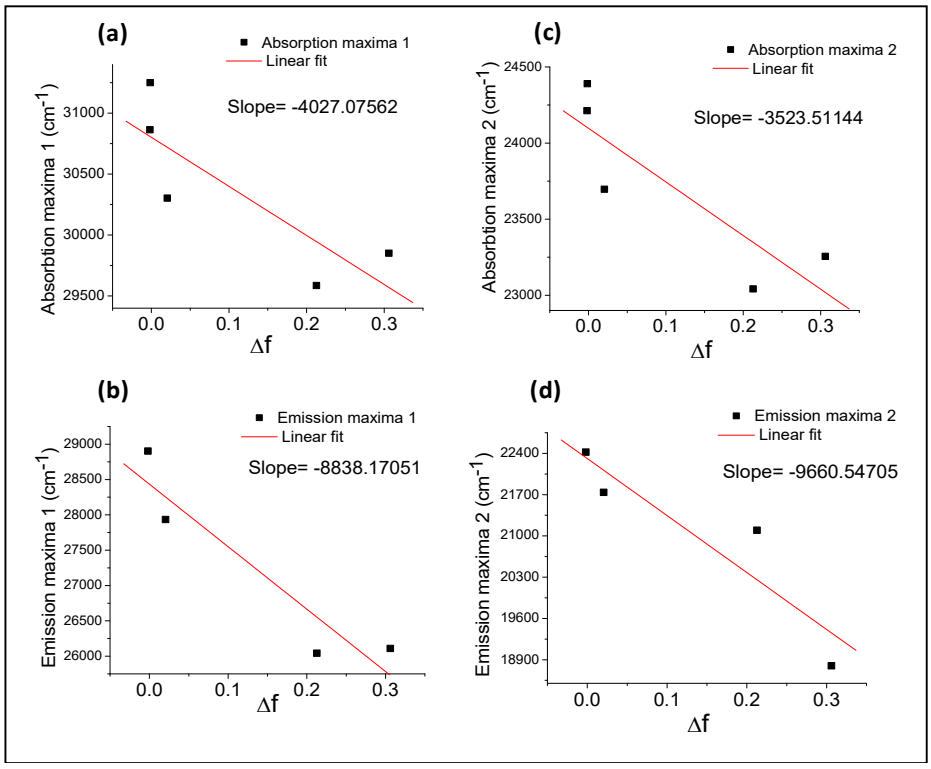

Figure 5. Plots of (a) absorption maxima 1, (b) emission maxima 1, (c) absorption maxima 2 and (d) emission maxima 2 against solvent polarity function Δf. Absorption and emission maxima are expressed in wavenumber (cm^{-1}).

One important difference between the two is that even though conformer 1 has a larger ground state dipole moment (μ_{g1}) than conformer 2 (μ_{g2}), the second conformer shows greater change in dipole moment than the first one, hence larger solvatochromism in the second conformer as observed. Therefore, based on the results presented so far, we have tentatively assigned conformer 1 as the planar conformer and conformer 2 as the twisted conformer. As we will see in the next section, this assignment is supported by computation.

Computational results

Optimized ground state geometry of structure **II** in vacuum using the DFT/B3LYP functional and 6–31G(d,p) basis set, is presented in Figure 6. The calculation predicted a planar geometry with a ground state dipole moment of 11.05 D. This value is in reasonable agreement with the experimental value 9.3 D. Frequency calculation at this geometry shows no imaginary frequency; hence it is a minimum structure.

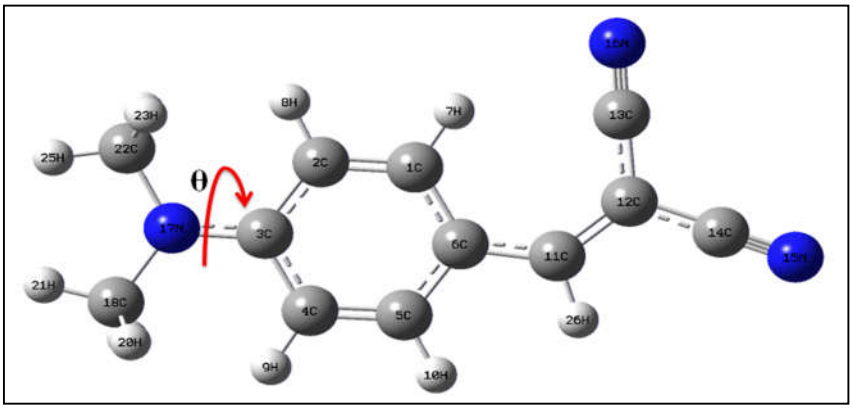

Figure 6. Optimized ground state geometry of structure **II** at calculated using DFT method at B3LYP/6–31G (d, p) level of the theory.

The same optimum ground state planar geometry is obtained in different solvents. However, the dipole moments show significant increments with increasing solvent polarity. The HOMO-LUMO band gap also shows bathochromic shift. The results are presented in Table 2.

Table 2. Calculated ground state energy, dipole moment and HOMO-LUMO gap of optimized ground state geometry of structure **II** at DFT/B3LYP/6–31G (d, p) level in solvents of different polarities.

Solvent	Energy (hartree)	ZPE (hartree)	E+ ZPE	LUMO-HOMO (eV)	Dipole moment (D)
Gas	-628.1198	0.204895	-627.9149	3.4743	11.0506
CHX	-628.7604	0.205034	-627.9210	3.3860	12.7648
DCM	-628.1331	0.205020	-627.9281	3.2958	14.7896
$CHCl_3$	-628.1310	0.205048	-627.9296	3.3272	14.1697
ACN	- 628.1351	0.204973	-627.9302	3.2727	15.3778

The UV-Visible spectrum of the twisted and planar conformers is computed in cyclohexane at TD-B3LYP/6-31G(d,p) level of the theory. The results are presented in Figures 7b and 7c, respectively. For comparison the absorption spectrum of structure **II** is also included in Figure 7a.

The calculated charge transfer band of the planar and twisted conformers shows a significant shift relative to the experiment. This is expected as no scaling factor is introduced in the calculation. One important prediction of the calculation is that a significant overlap of the absorption bands of the two forms is possible and hence co-excitation of the two forms. The solvatochromic response of the twisted conformer is greater than that of the planar one despite the fact that the latter has slightly smaller dipole moment (i.e. 9.3 D for the planar versus 7.1 D for the twisted conformer). This observation was explained in earlier based on the changes in the

dipole moments associated with the excitation of each conformer. In this case, the twisted conformer shows greater change in dipole moment upon excitation and hence greater solvatochromism. This argument is further supported by frontier orbital analyses of the two conformers presented in Figure 8. The analyses suggests that HOMO-LUMO excitation results in a shift of the electron density from the dimethylaminomoiety to the dicyanovinyl group in both conformers. However, the charge transfer is more pronounced in the twisted conformer in line with the more charge transfer character of the red-shifted absorption and emission observed in polar solvents.

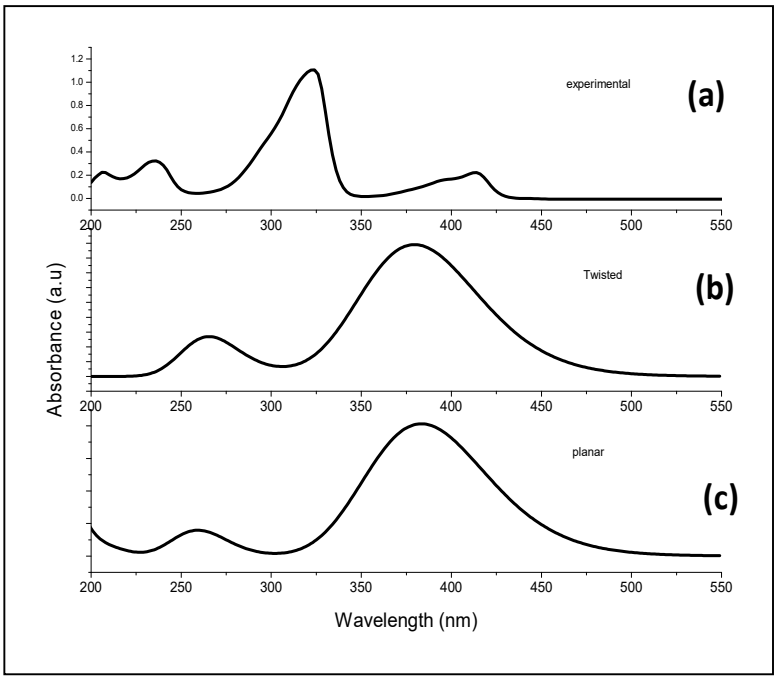

Figure 7. Experimental (a) and calculated absorption spectrum of twisted (b) and planar (c) conformers of structure **II**. The experimental absorption spectrum was in cyclohexane. The calculation of vertical excitation was performed using TD-DFT method, B3LYP functional and 6-31G(d,p) basis set.

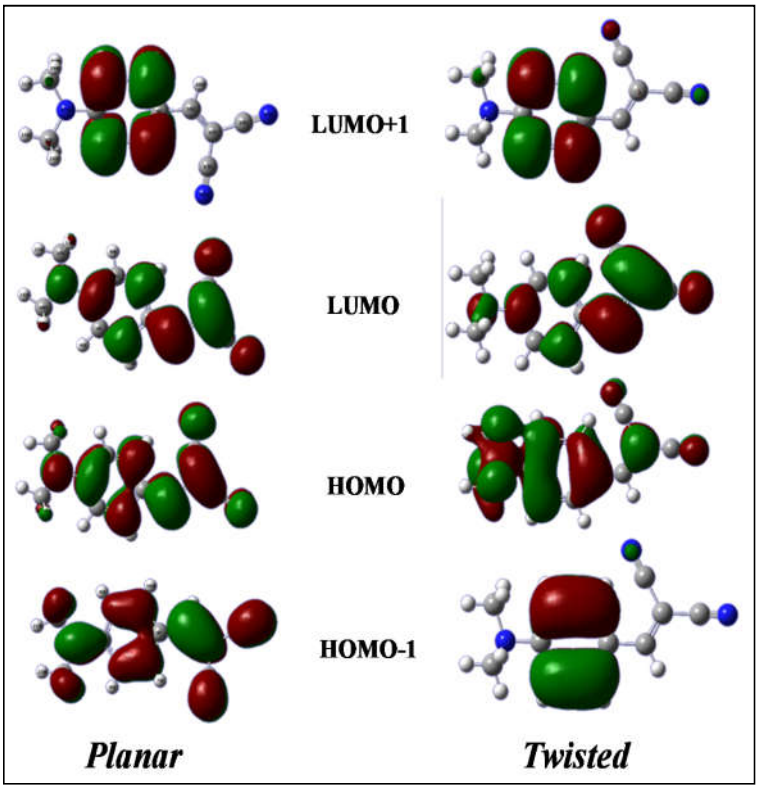

Figure 8. Frontier molecular orbitals of the planar (left panel) and twisted (right panel) of structure **II** calculated by DFT method using B3LYP functional and 6-31G(d,p) basis set.

CONCLUSION

In this study, dual fluorescence property of structure **II** (*p*-N,N-(dialkylamino) benzylidenemalononitrile) was investigated by steady-state absorption and fluorescence studies. Solvatochrmoic properties of the absorption and emissions were also reported. Analyses of the excitation wavelength and solvent polarity dependence of the emission spectra showed that the compound consists of two conformational isomers which are also supported by theoretical computation. The results presented so far confirm the existence of twisted ground state fluorophore which is responsible for the second emission band in the dual fluorescence of structure **II**. Hence, direct access to the emitting TICT state is possible. The results are also supported by a comparative study of structurally related compounds, structures **I** and **III**. The existence and solvent control of TICT conformers in push-pull systems have important implications on technologies such as ICT-induced charge transport modulations in junctions. Our conclusion of the presence of two stable ground state conformers of structure **II** could be further verified by temperature-dependent UV-Vis, IR and jet-cooled laser-induced fluorescence (LIF) studies. Since the equilibrium population of the two conformers will be temperature-dependent, their corresponding UV-Vis and IR signals are also expected to be temperature-dependent.

ACKNOWLEDGEMENTS

The Research and Extension Office of Haramaya University (HURG-2014-03-03), Postgraduate Program Directorate and Chemistry Department of Haramaya University are greatly acknowledged. D.G. Woldegiorgis acknowledges the financial support from Mr. Girma Juhar.

REFERENCES

1. Wagner, N.L.; Greco, J.A.; Enriquez, M.M.; Frank, H.A.; Birge, R.R. The nature of the intramolecular charge transfer state in peridinin. *Biophys. J.* **2013**, 104, 1314-1325.
2. El-Zohry, A.M.; Karlsson, M. Gigantic relevance of twisted intramolecular charge transfer for organic dyes used in solar cells. *J. Phys. Chem. C* **2018**, 122, 23998-24003.
3. Gharaati, A.; Abed, Y.; Mostaghni, F. Nonlinear optical characteristics of N,N'-bis (salicylidene)-*p*-phenylenediamine: Z-scan technique and quantum mechanical calculations. *Bull. Chem. Soc. Ethiop.* **2022**, 36, 465-477.
4. Hoogesteger, F.J.; van Walree, C.A.; Jenneskens, L.W.; Roest, M.R.; Verhoeven, J.W.; Schuddeboom, W.; Piet, J.J.; Warman, J.M. Photoinduced intramolecular charge separation in donor/acceptor ‑ substituted bicyclohexylidene and bicyclohexyl. *Chem. Eur. J.* **2000**, 6, 2948-2959.
5. Samanta, P.K.; Misra, R. Intramolecular charge transfer for optical applications. *J. Appl. Phys.* **2023,** 133, 020901.
6. Zong, C.; Lu, Q.; Niu, J.; Meng, F.; Yu, X. A fluorescent probe for detecting mitochondrial viscosity and its application in distinguishing human breast cancer cells from normal ones. *Spectrochim. Acta, Part A* **2023**, 299, 122883.
7. Lippert, E.; Lüder, W.; Moll, F.; Nägele, W.; Boos, H.; Prigge, H. Seibold-Blankenstein, Umwandlung von elektronenanregungsenergie. *Angew. Chem.* **1961**, 73, 695-706.
8. Kasha, M. Characterization of electronic transitions in complex molecules. *Discuss. Faraday Soc.* **1950**, 9, 14-19.
9. Grabowski, Z.R.; Rotkiewicz, K.; Rettig, W. Structural changes accompanying intramolecular electron transfer: focus on twisted intramolecular charge-transfer states and structures. *Chem. Rev.* **2003**, 103, 3899-4032.
10. Karpiuk, J. Dual fluorescence from two polar excited states in one molecule. Structurally additive photophysics of crystal violet lactone. *J. Phys. Chem. A* **2004**, 108, 11183-11195.
11. Rettig, W.; Chandross, E.A. Dual fluorescence of 4,4'-dimethylamino-and 4,4'-diaminophenyl sulfone. Consequences of d-orbital participation in the intramolecular charge separation process. *J. Am. Chem. Soc*. **1985**, 107, 5617-5624.
12. Cazeau-Dubroca, C.; Ait Lyazidi, S.; Cambou, P.; Peirigua, A.; Cazeau, P.; Pesquer, M. Twisted internal charge transfer molecules: already twisted in the ground state. *J. Phys. Chem.* **1989**, 93, 2347-2358.
13. Cazeau-Dubroca, C.; Peirigua, A.; Lyazidi, S.A.; Nouchi, G.; Cazeau, P.; Lapouyade, R. TICT fluorescence in rigid matrices: α-delayed fluorescence. *Chem. Phys. Lett.* **1986**, 124, 110-115.
14. Visser, R.J.; Varma, C.A.; Konijnenberg, J.; Bergwerf, P. Solute–solvent exciplex versus twisted intramolecular charge-transfer state in anomalous fluorescence of 4-N,N-dimethylaminobenzonitrile. *J. Chem. Soc. Faraday Trans. II* **1983**, 79, 347-367.
15. Grabowski, Z.R. Twisted intramolecular charge transfer states (Tict): A new class of excited states with a full charge separation. *New J. Chem.* **1979**, 3, 443-454.
16. Herbich, J.; Perez Salgado, F.; Rettschnick, R.P.; Grabowski, Z.R.; Wojtowicz, H. " Twisted" intramolecular charge-transfer states in supercooled molecules: structural effects and clustering with polar molecules. *J. Phys. Chem.* **1991**, 95, 3491-3497.

17. Rotkiewicz, K.; Grellmann, K.; Grabowski, Z. Reinterpretation of the anomalous fluorescense of pn, n-dimethylamino-benzonitrile. *Chem. Phys. Lett.* **1973**, 19, 315-318.
18. Dobkowski, J.; Rettig, W.; Waluk, J. Intramolecular charge-transfer properties of a molecule with a large donor group: the case of 4′-(pyren-1-yl) benzonitrile. *Phys. Chem. Chem. Phys.* **2002**, 4, 4334-4339.
19. Zachariasse, K.A. Comment on "Pseudo-Jahn–Teller and TICT-models: a photophysical comparison of meta-and para-DMABN derivatives" [*Chem. Phys. Lett.* **1999**, 305, 8]: The PICT model for dual fluorescence of aminobenzonitriles. *Chem. Phys. Lett.* **2000**, 320, 8-13.
20. Zachariasse, K.; Grobys, M.; Von der Haar, T.; Hebecker, A.; Il'Ichev, Y.V.; Jiang, Y.-B.; Morawski, O.; Kühnle, W. Intramolecular charge transfer in the excited state. Kinetics and configurational changes. *J. Photochem. Photobiol. A* **1996**, 102, 59-70.
21. Zachariasse, K.A.; von der Haar, T.; Hebecker, A.; Leinhos, U.; Kuhnle, W. Intramolecular charge transfer in aminobenzonitriles: Requirements for dual fluorescence. *Pure Appl. Chem.* **1993**, 65, 1745-1750.
22. Hochstrasser, R.M.; Marzzacco, C. Electronic spectra of molecules with nearby electronic states. *Mol. Lumin.* **1969**, 631-655.
23. Duben, A.; Goodman, L.; Koyanagi, M. In Excited States; Lim, E.C. (Ed.), Academic Press: New York; **1974**.
24. Yoshihara, T.; Druzhinin, S.I.; Zachariasse, K.A. Fast intramolecular charge transfer with a planar rigidized electron donor/acceptor molecule. *J. Am. Chem. Soc.* **2004**, 126, 8535-8539.
25. Atsbeha, T.; Mohammed, A.M.; Redi-Abshiro, M. Excitation wavelength dependence of dual fluorescence of DMABN in polar solvents. *J. Fluoresc.* **2010**, 20, 1241-1248.
26. Hussien, N.A.; Mohammed, A.M.; Tessema, M.; Dejene, F.; Redi-Abshiro, M. Solvent polarity and excitation wavelength dependence of the dual fluorescence in N,N-diethyl-4-nitrosoaniline. *J. Fluoresc.* **2012**, 22, 451-456.
27. Gemeda, F.; Redi-Abshiro, M.; Mustefa, A. Excitation wavelength dependence of dual fluorescent molecules. *Int. Res. J. Pure Appl. Chem.* **2016**, 13, 1-15.
28. Mengesha, E.T.; Demissie, T.B.; Redi-Abshiro, M.; Mohammed, A.M. Dual fluorescence of (E)-N-(4-(dimethylamino) benzylidene)-2H-1,2,4-triazol-3-amine (DMABA-Amtr): A ground state perspective. *Spectrochim. Acta Part A* **2018**, 189, 601-607.
29. Yasini, P.; Shepard, S.; Smeu, M.; Borguet, E. Modulation of charge transport through single molecules induced by solvent-stabilized intramolecular charge transfer. *J. Phys. Chem. B* **2023**, 127, 9771-9780.
30. Jin, H.; Liang, M.; Arzhantsev, S.; Li, X.; Maroncelli, M. Photophysical characterization of benzylidene malononitriles as probes of solvent friction. *J. Phys. Chem. B* **2010**, 114, 7565-7578.
31. Haidekker, M.; Brady, T.; Lichlyter, D.; Theodorakis, E. Effects of solvent polarity and solvent viscosity on the fluorescent properties of molecular rotors and related probes. *Bioorg. Chem.* **2005**, 33, 415-425.
32. Kung, C.E.; Reed, J.K. Microviscosity measurements of phospholipid bilayers using fluorescent dyes that undergo torsional relaxation. *Biochem.* **1986**, 25, 6114-6121.
33. Deb, M.L.; Bhuyan, P.J. Uncatalysed Knoevenagel condensation in aqueous medium at room temperature. *Tetrahedron Lett.* **2005**, 46, 6453-6456.
34. Patil, S.S.; Jadhav, S.D.; Deshmukh, M. Eco-friendly and economic method for Knoevenagel condensation by employing natural catalyst. *Indian J. Chem.* **2013**, 52B, 1172-1175.
35. Sharghi, H.; Ebrahimpourmoghaddam, S.; Doroodmand, M.M. Iron-doped single walled carbon nanotubes as an efficient and reusable heterogeneous catalyst for the synthesis of organophosphorus compounds under solvent-free conditions. *Tetrahedron* **2013**, 69, 4708-4724.
36. Frisch, M.; Trucks, G.; Schlegel, H.; Scuseria, G.; Robb, M.; Cheeseman, J.; Scalmani, G.; Barone, V.; Mennucci, B.; Petersson, G. Gaussian 09, revision A. 02, Gaussian, Inc.,

Wallingford, CT, 2009 Search PubMed; (b) C. Lee, W. Yang and RG Parr. *Phys. Rev. B: Condens. Matter Mater. Phys.* **1988**, 37, 785.
37. Beeke, A.D., Density-functional thermochemistry. III. The role of exact exchange. *J. Chem. Phys.* **1993**, 98), 5648-5652.
38. Lee, C.; Yang, W.; Parr, R.G., Development of the Colle-Salvetti correlation-energy formula into a functional of the electron density. *Phys. Rev. B* **1988**, 37, 785.
39. Stratmann, R.E.; Scuseria, G.E.; Frisch, M.J. An efficient implementation of time-dependent density-functional theory for the calculation of excitation energies of large molecules. *J. Chem. Phys*. **1998**, 109, 8218-8224.
40. Catalan, J.; Del Valle, J.C. A spectroscopic rule from the solvatochromism of aromatic solutes in nonpolar solvents. *J. Phys. Chem. B* **2014**, 118, 5168-5176.
41. Reichardt, C. Solvatochromic dyes as solvent polarity indicators. *Chem. Rev.* **1994**, 94, 2319-2358.
42. Reichardt, C. Solvents and solvent effects: An introduction. *Org. Process Res. Dev.* **2007**, 11, 105-113.
43. Marini, A.; Munoz-Losa, A.; Biancardi, A.; Mennucci, B. What is solvatochromism? *J. Phys. Chem. B* **2010**, 114, 17128-17135.
44. Lippert, E. Dipolmoment und elektronenstruktur von angeregten molekülen. *Z. Naturforsch*. **1955**, 10, 541-545.
45. Mataga, N.; Kaifu, Y.; Koizumi, M. Solvent effects upon fluorescence spectra and the dipolemoments of excited molecules. *Bull. Chem. Soc. Jpn.* **1956**, 29, 465-470.
46. Sıdır, İ.; Sıdır, Y.G.; Berber, H.; Demiray, F. Emerging ground and excited state dipole moments and external electric field effect on electronic structure. A solvatochromism and theoretical study on 2-((phenylimino) methyl) phenol derivatives. *J. Mol. Liq.* **2015**, 206, 56-67.
47. Demissie, E.G.; Mengesha, E.T.; Woyessa, G.W., Modified solvatochromic equations for better estimation of ground and excited state dipole moments of p-aminobenzoicacid (PABA): Accounting for real shape over hypothetical spherical solvent shell. *J. Photochem. Photobiol. A* **2017**, 337, 184-191.